Available online at www.sciencedirect.com
SCIENCE DIRECT
Journal of Colloid and Interface Science 283 (2005) 215–222
JOURNAL OF Colloid and Interface Science
www.elsevier.com/locate/jcis

Effect of electric fields on contact angle and surface tension of drops

A. Bateni [a], S. Laughton [a], H. Tavana [a], S.S. Susnar [a], A. Amirfazli [b], A.W. Neumann [a,*]

[a] *Department of Mechanical and Industrial Engineering, University of Toronto, Toronto, ON M5S 3G8, Canada*
[b] *Department of Mechanical Engineering, University of Alberta, Edmonton, AB T6G 2G8, Canada*

Received 2 April 2004; accepted 18 August 2004

Available online 30 November 2004

Abstract

Contact angles of sessile drops were experimentally investigated in the electric field. The experimental setup was designed such that the electric field was applied to all three interfaces. The advanced Automated Polynomial Fitting (APF) methodology was employed to measure contact angles with high accuracy. The significance of the observations and trends was examined by conducting statistical tests of hypothesis. It was found that contact angles of polar liquids such as alcohols increase in the electric field. However, no significant trend was observed for nonpolar liquids such as alkanes. The change in the contact angle was found to be stronger for liquids with longer molecules. It was shown that the polarity of the electric field is not an underlying factor in the observed trends. Using the equation of state for interfacial tensions, the observed shift in contact angles was translated into a corresponding change in surface tension of the liquids. The results suggest that the surface tension of alcohols increases by one to two percent (depending on the size of molecules) when an electric field of the order of magnitude of 10^6 V/m is applied.

Keywords: Contact angle; Surface tension; Electric field; Sessile drops; Automated Polynomial Fitting (APF)

1. Introduction

Charged or electrified drops play an important role in many technologies, such as inkjet printing [1], electrostatic painting and spraying [2–7], chemical and physical separations [8–12], agricultural treatments [13,14], and electrostatic gas cleaning [15]. The fact that an electrostatic field can modify drop properties, such as surface tension and contact angle, is of great importance from both practical and fundamental points of view. Further development of new technologies in the above areas requires a thorough understanding of the effects of the electric field on any of these properties.

Many researchers have studied the shape and stability of drops in electric fields [16–20]. Contact angle phenomena in the electric field have also been of interest for a long time [21–23]. This subject received renewed attention recently because of its application in electrowetting [24–31]. The majority of the recent work considered a configuration in which the electric field was applied only to the solid–liquid interface. That is, the voltage was applied between the liquid and a conducting layer underlying the solid surface. These studies have shown that using the above configuration the electric field deforms the drop and reduces the contact angle. In these studies, it was generally assumed that the liquid–vapor and solid–vapor surface tensions, i.e., γ_{lv} and γ_{sv}, are unaffected by the electric field, and the observed change in the contact angle is a consequence of a decrease in the solid–liquid surface tension, γ_{sl} [24–29]. The Lippmann equation [32] is often used to describe the effect of the electric field on γ_{sl} and hence on the contact angle. However, Digilov [24] argued that the Lippmann equation only qualitatively explains the observed change in the contact angle. He suggested that the decrease in the contact angle is caused by the reduction of line tension due to the redistribution of charges on the three phase contact line. The size of

* Corresponding author. Fax: +1(416)-978-7753.
E-mail address: neumann@mie.utoronto.ca (A.W. Neumann).

0021-9797/$ – see front matter
doi:10.1016/j.jcis.2004.08.134

the drops in the present study was chosen so that the effect of line tension on contact angle is negligible.

Despite the conceptual simplicity, experience has shown that the measurement and thermodynamic interpretation of contact angles is not a trivial task. The accuracy of the results in contact angle measurements can be affected by the quality of the solid surface, the purity of the test liquids, the skill of the experimenter, and most importantly the methodology used [33,34]. Therefore, when contact angle phenomena are the focus of attention, particular requirements must be met to produce thermodynamically significant results [35]. Most importantly, advancing contact angles must be measured and interpreted [35,36]. By employing such an approach problems such as contact angle hysteresis, slip and stick of the three-phase line, and solid–liquid interactions can be discovered and resolved. It is not evident whether appropriate conditions were used in previous reports. Therefore, it was decided to investigate contact angle phenomena in electric fields, so that it can be interpreted from the thermodynamic point of view. Performing such contact angle measurements can also be an effective approach to infer information about liquid surface tensions in the electric field.

Understanding the effect of an electric field on surface tension of drops is a secondary purpose of this study. This effect has been studied by several authors [37–45]; however, no general agreement can be found in the results. Liggieri et al. [43] developed a theoretical model based on the Maxwell stress tensor to predict the effect of an electric/magnetic field on the surface tension of liquids. They concluded that such effects would be small and negligible for spherical drops. On the other hand, Sato et al. [44] conducted an experimental study and reported that the surface tension of liquids (e.g., water, salt water, and alcohols) can be decreased significantly in the presence of an electric field, depending on the conductivity of the liquid. Bateni et al. [37] recently developed a new drop-shape methodology, called Axisymmetric Drop Shape Analysis—electric field, to measure the effect of an electric field on the surface tension of drops. Their early results suggested that the surface tension of distilled water increases by about 2% in an electric field of the order of magnitude of 10^6 V/m. Thus it is apparent that further investigation is required to bring about clarity in this area. In this study the effect of electric fields on the surface tension was calculated from the corresponding change in the contact angle. The equation of state for interfacial tensions was employed along with the Young equation to perform these calculations.

The experimental setup proposed in this study is shown in Fig. 1. In this configuration the drop is formed within a parallel plate capacitor so that all interfaces are exposed to the electric field. No assumptions were made in this study regarding liquid–vapor, γ_{lv}, or solid–liquid, γ_{sl}, surface tensions. Also it should be noted that the Lippmann equation is not applicable to the configuration used in this study, since the observed change in the contact angles cannot be explained merely by a change in solid–liquid surface tension γ_{sl}.

2. Materials and methodology

A series of experiments were conducted using alcohols and alkanes on Teflon-coated silicon wafers in the electric field. Contact angles of six alcohols, hexanol, heptanol, octanol, nonanol, decanol, and dodecanol, and two alkanes, decane and hexadecane, were investigated.

Teflon AF 1600 was chosen as a coating material because of its exceptional electrical, mechanical, and chemical properties [46,47]. A 6% solution of Teflon AF 1600 in Fluorinert FC-75 (the solution is referred to as Teflon AF 1601S) was purchased from Dupont Co. (London, ON) and used as coating liquid. Silicon wafers with a thickness of 525 ± 50 μm were used as the substrate because of their smoothness, rigidity, and high surface tension. The latter property causes the polymeric solution to spread uniformly on the surface during the coating process [48]. The silicon wafers were coated using a dip-coating technique [49]: the wafers were cleaned by sonication in ethanol and then distilled water and dried under a heat lamp. Next, the substrates were immersed vertically into and then emersed out of the coating solution at a constant low speed. The coated surfaces were then dried at room temperature. Our preliminary experiments showed that careful preparation of solid samples according to the above procedure is necessary to detect the patterns reported in this paper.

The coated silicon wafer was placed on the lower plate of a capacitor such that the stainless needle passes through the hole in the center of the substrate (see Fig. 1). The needle was used to form the drop and control its volume without distorting the liquid–vapor interface. The needle was connected to a motor-driven syringe and a stepper motor controller (Model 18705, Oriel Instruments, CT). Teflon tape was wrapped around the needle to prevent leakage of liquid between the needle and the hole.

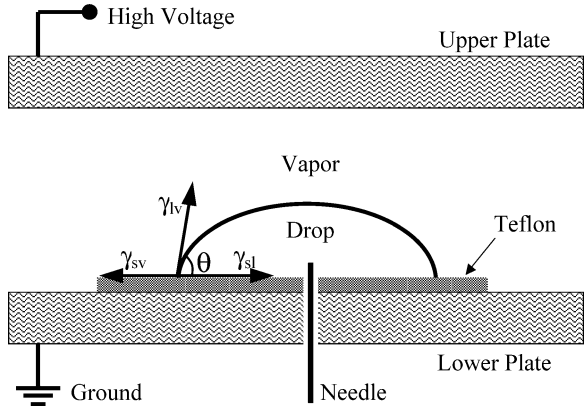

Fig. 1. The schematic of the experimental configuration used in this study. The drop is formed within a parallel-plate capacitor on a Teflon-coated substrate.

The capacitor was made of two parallel discs with a radius of 30 mm (see Fig. 1). The plates of the capacitor were made of copper. The upper disc of the capacitor was connected to a high-voltage power supply and the lower disc and the needle were grounded. The body of the electric field cell (not shown in Fig. 1) was manufactured from Delrin, a light polymer which is a good electrical insulator and chemically inert. A distance of 6 mm was used between the two plates in all the experiments reported here.

The drop was illuminated by a light source (Model V-WLP1000, Newport Corp., Fountain Valley, CA). The images were acquired using a system consisting of a microscope (Apozoom, Leitz Wetzlar, Germany), a CCD camera (Model 4815-5000, Cohu Co.), and a digital video processor (Parallax Graphics, CA); image resolution is 640 by 480 with 256 grey levels.

An Automated Polynomial Fitting (APF) technique was used to process the images [50]. APF was developed recently to measure local contact angles with high accuracy. Unlike other high-accuracy techniques (e.g., Axisymmetric Drop Shape Analysis), no assumption with respect to shape or density of drops was made in APF, which is thus applicable quite universally [50].

The APF method acquires high-magnification (e.g., 35×) images from a contact point of a drop (see Fig. 2). Since the whole drop does not fit into a magnified image, images are taken from either the right or left side of the drop. Then the drop profile is extracted using image-processing techniques. The drop contact point (i.e., the point where the three interfaces meet) is detected automatically. A polynomial is fitted to the experimentally observed drop profile and the contact angle is calculated from the slope of the polynomial at the contact point. Sophisticated statistical analysis was carried out to determine the optimum parameters for the curve fitting, e.g., the order of the polynomial and the number of pixels used in the fitting procedure. It was reported that for the current configuration the optimum accuracy was achieved when third-order polynomials were fitted to a series of 130 pixels of the drop profile next to the contact point. Details of this methodology can be found elsewhere [50].

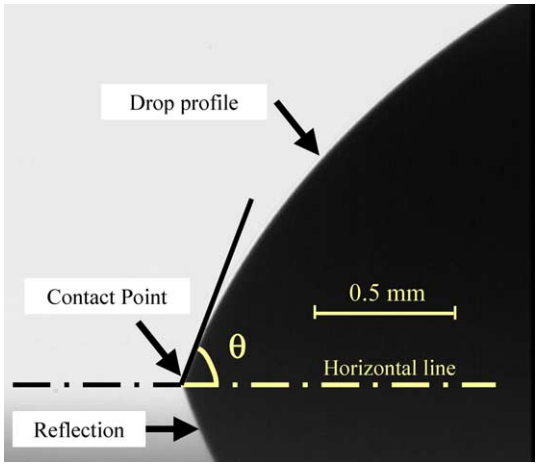

Fig. 2. A typical high-magnification (35×) image acquired from the left side of a sessile drop of heptanol on Teflon. The cusp angle is the result of the reflection of the drop image at the solid surface.

Low-rate dynamic contact angles were measured over time in this study. An initial drop was formed at the beginning of each run of experiment. The motorized syringe was then operated at a constant rate. Liquid was pumped into the drop so that the three-phase line advances with a speed of about 1 mm/min. It is well known that the liquid flow of this rate does not affect the contact angle [35,36]. Images were taken with a frequency of 1 image/s. In total 40 images were acquired and analyzed by APF during each run (i.e., 20 images from each side of the drop). Then the images were processed by the APF technique as mentioned above, so that one contact angle measurement is obtained form each image. The diameter of the drop during experiments was kept in the range of 6 to 8 mm to ensure that the effect of line tension is negligible in the results. Experiments with suspended glass beads were conducted to investigate the possibility of an induced liquid flow in the drop due to the applied electric field. It was found that the glass beads of 70–105 and 45–62 μm suspend fairly well in water and alcohol, respectively. No significant flow was detected within the range of electric potentials used in this study. All experiments were conducted at ambient temperature, i.e., $24.5° \pm 0.5°$, and a relative humidity of about 50%.

3. Results and discussion

Contact angle measurements were conducted at electric potentials ranging from 0 to 4 or 5 kV (depending on the liquid). Applying higher voltages was not possible due to the stability limit of the drop. With the geometries under consideration, a voltage of 5 kV creates the electric field of about 8.3×10^5 V/m within the capacitor far from the drop. Previous studies [37] have shown that the magnitude of the electric field is at a maximum at the drop apex (i.e., 3–5 times higher than the above value) and is at a minimum at the three-phase line.

At each electric potential, nine runs of experiments (replications) were performed. A new solid sample was used for each run to ensure that the results are not biased due to the solid samples. As mentioned above, each run consists of 40 observations. The results of each run were graphed and carefully examined. Fig. 3 shows the result of a typical run of experiment for heptanol on Teflon at zero electric field. The graph is expected to be fairly uniform and independent of time. Any observation outside the three-sigma limit was removed. Whenever a trend or pattern was observed in the results the run was rejected and repeated. Such patterns can be a consequence of solid–liquid interactions, slip–stick of the three-phase line, or a low-quality solid sample [35,36].

The observations of each run were averaged and considered as a single data point for the further calculations (see Fig. 3). The overall mean and confidence interval at each

voltage was then calculated from the resulting nine data points. Table 1 shows the summary of the results and calculations for contact angles of octanol in the electric field. Similar calculations were performed for all the liquids under study. Table 2 shows the overall mean and 95% confidence intervals for the contact angles of these liquids at different voltages. The results of Table 2 suggest that the contact angles generally increase from left to right at each row, i.e., with increasing magnitude of the applied potential.

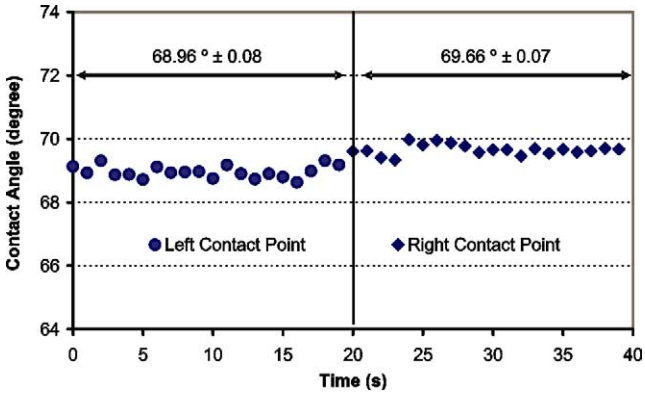

Fig. 3. Results of a typical run of experiments: heptanol on Teflon at zero electric field. The slight difference between right and left contact angles suggests that the drop was not perfectly axisymmetric. The total average of the run (including both right and left observations) was calculated as $69.31° \pm 0.12°$. This value was used for the further statistical calculations.

Analysis of linear regression was performed to further investigate the significance of the observed trend in the contact angles [51]. For each liquid, a regression line was fitted to the results shown in Table 2. The 95% confidence limits were calculated for the slope and intercept of each regression line. The goodness of the linear model was examined by calculating the correlation coefficient, R^2, for each liquid.

Table 3 shows the calculated slope, intercept, and correlation coefficient for each of the liquids under consideration. High values (close to one) for the correlation coefficients of alcohols validate the linear model for these liquids. It should be noted that the validity of the linear model does not signify that the physical relation of the two variables is indeed linear. It only suggests that within the range of electric potentials considered in this study a first-order approximation provides sufficient accuracy. Fig. 4 shows the graphical representation of the results (i.e., overall means) for alcohols along with the fitted regression lines.

The calculated slopes in contact angles might be merely a consequence of random experimental error. Hence, the significance of these values must be examined using statistical test of hypothesis. The null hypothesis of H_0: SLOPE $= 0$ was tested versus H_1: SLOPE > 0 for each liquid. The variation of the experimental error around the regression line (i.e.,

Table 1
Summary of the contact angle results for octanol on Teflon in the electric field

Replications	Applied electric potential (kV)				
	0	1	2	3	4
Run 1	71.19 ± 0.11	71.07 ± 0.12	71.39 ± 0.09	71.63 ± 0.11	71.66 ± 0.13
Run 2	71.20 ± 0.12	71.23 ± 0.10	71.38 ± 0.08	71.27 ± 0.10	71.73 ± 0.13
Run 3	71.14 ± 0.07	71.15 ± 0.12	71.27 ± 0.11	71.41 ± 0.13	71.73 ± 0.11
Run 4	70.85 ± 0.08	71.21 ± 0.11	71.20 ± 0.07	71.53 ± 0.10	71.59 ± 0.07
Run 5	70.95 ± 0.05	71.34 ± 0.07	71.45 ± 0.09	71.57 ± 0.22	71.70 ± 0.13
Run 6	71.22 ± 0.10	71.20 ± 0.10	71.32 ± 0.11	71.51 ± 0.13	71.82 ± 0.11
Run 7	70.95 ± 0.07	70.98 ± 0.09	71.51 ± 0.09	71.50 ± 0.07	71.54 ± 0.13
Run 8	70.73 ± 0.08	71.25 ± 0.08	71.17 ± 0.10	71.50 ± 0.11	71.46 ± 0.09
Run 9	72.00 ± 0.12	71.16 ± 0.11	71.28 ± 0.11	71.50 ± 0.08	71.47 ± 0.10
Overall mean	71.14 ± 0.24	71.18 ± 0.07	71.33 ± 0.07	71.49 ± 0.07	71.63 ± 0.08

Note. Each entry shows the average and 95% confidence interval for a run. The overall mean and confidence intervals for each voltage were calculated from the nine replications.

Table 2
Overall mean and confidence interval of contact angle of alcohols and alkanes in the electric field

Liquid	Applied electric potential (kV)						
	0	1	2	3	4	4.5	5
Hexanol	68.20 ± 0.11	68.27 ± 0.10	68.40 ± 0.11	68.47 ± 0.10	68.59 ± 0.15	68.60 ± 0.15	–
Heptanol	69.47 ± 0.18	69.92 ± 0.52	69.57 ± 0.18	69.71 ± 0.17	70.02 ± 0.18	70.09 ± 0.25	–
Octanol	71.14 ± 0.24	71.18 ± 0.07	71.33 ± 0.07	71.49 ± 0.07	71.63 ± 0.08	–	–
Nonanol	71.90 ± 0.08	71.92 ± 0.05	72.10 ± 0.12	72.12 ± 0.13	72.42 ± 0.06	72.54 ± 0.15	–
Decanol	73.07 ± 0.14	73.23 ± 0.17	73.33 ± 0.13	73.55 ± 0.17	73.77 ± 0.20	–	73.91 ± 0.23
Dodecanol	74.50 ± 0.24	74.70 ± 0.19	74.86 ± 0.21	75.07 ± 0.25	75.24 ± 0.22	75.47 ± 0.22	–
Decane	57.95 ± 0.19	58.03 ± 0.21	57.87 ± 0.10	58.00 ± 0.21	57.92 ± 0.16	–	58.18 ± 0.22
Hexadecane	68.77 ± 0.18	68.56 ± 0.13	68.61 ± 0.10	68.69 ± 0.19	68.63 ± 0.17	–	68.53 ± 0.20

Note. Each data point was calculated from nine replications as shown in Table 1. The results suggest an increase in contact angles with increasing applied electric potential.

Table 3
Slope, intercept and correlation coefficient, R^2, of the regression line for alcohols and alkanes

Liquid	Slope	Intercept	R^2	t_0	$t_{\alpha;n-2}$	Test result
Hexanol	0.09 ± 0.01	68.19 ± 0.04	0.99	19.35	2.13	Significant
Heptanol	0.11 ± 0.14	69.54 ± 0.40	0.55	2.19	2.13	Significant
Octanol	0.13 ± 0.04	71.09 ± 0.10	0.97	10.06	2.35	Significant
Nonanol	0.14 ± 0.06	71.82 ± 0.19	0.91	6.22	2.13	Significant
Decanol	0.17 ± 0.02	73.05 ± 0.07	0.99	20.05	2.13	Significant
Dodecanol	0.20 ± 0.04	74.48 ± 0.10	0.98	16.03	2.13	Significant
Decane	0.03 ± 0.07	57.93 ± 0.23	0.20	1.01	2.13	Not significant
Hexadecane	-0.03 ± 0.05	68.70 ± 0.17	0.31	-1.35	2.13	Not significant

Note. The last three columns show the calculation and results of the statistical test of hypotheses to examine the significance of the slopes. The slope is significant at the 95% confidence level only for alcohols.

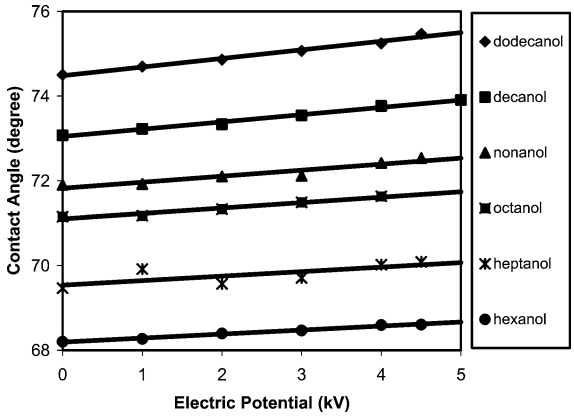

Fig. 4. Graphical representation of contact angles of alcohols in the electric field. Each data point indicates the overall mean of measurements shown in Table 2.

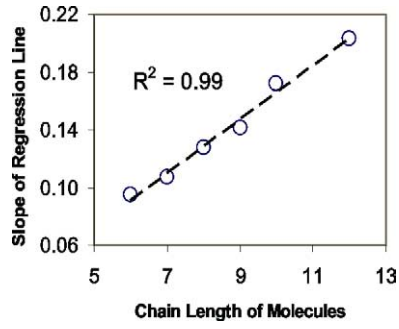

Fig. 5. Slope of the regression line, describing the contact angle of alcohols in electric field, versus the chain length of molecules. The graph suggests that the effect of electric field on contact angle of alcohols increases with increasing size of the molecules.

the model variance) was estimated by [51]

$$S^2 = \sum_{i=1}^{n} \frac{(\theta_i^{\text{obs}} - \theta_i^{\text{est}})^2}{n-2}, \tag{1}$$

where θ^{obs} and θ^{est} are the observed and estimated (from regression line) contact angles, respectively, and n is the number of observations (number of different voltages studied). Next, the statistic t_0 can be calculated as

$$t_0 = \frac{\text{SLOPE}^{\text{obs}}}{S} \sqrt{\sum_{i=1}^{n} (V_i - \bar{V})^2}, \tag{2}$$

where $\text{SLOPE}^{\text{obs}}$ is the calculated slope of the regression line (see Table 3) and V_i is the applied electric potential. The null hypothesis was rejected when the calculated statistic is larger than the value of the t-distribution with $n-2$ degrees of freedom and 95% confidence limit (i.e., $t_0 > t_{0.05;n-2}$).

The last three columns of Table 3 summarize the results of the above statistical calculations. The results indicate that the positive slopes observed for alcohols are significant, with a confidence limit of 95%. However, the slopes calculated for alkanes are not significant and can be merely a consequence of random experimental errors. Hence it can be concluded that the polarity of the liquids plays a key role in the observed increase in the contact angles.

By further scrutinizing the results in Table 3, it turns out that the slopes are larger for the alcohols with longer molecules. That is, the contact angles of alcohols with longer chain molecules are more sensitive to the applied electric field. This finding is graphically demonstrated in Fig. 5.

The effect of the direction of the electric field was also investigated by reversing the polarity of the capacitor and repeating the experiment for octanol. Using linear regression analysis (i.e., Eqs. (1) and (2)) a statistically significant slope of 0.13 was obtained (details of the results and calculations are not shown here). This slope is in the same direction and magnitude of the corresponding value in Table 3, suggesting that the direction of the electric field does not play a significant role in the observed effect of the electric field on contact angles. Similar conclusions were drawn earlier regarding the shape [52] and surface tension [44] of drops in the electric field.

It should be noted that by employing the Young–Lippmann equation [24,25,31] one would predict a decrease in contact angles as a result of the applied electric field, which is clearly contrary to the experimental findings reported in Table 3. The reason for this contradiction is that in the Lippmann equation it was assumed that there is no charge density/electric field at the liquid–fluid interface. Consequently γ_{lv} is assumed to remain unchanged in the electric field. However, it is known that this is not a valid assumption for the experimental setup used in this study. In fact, the distri-

bution of the electric field along the drop surface was calculated previously for similar configurations (see Ref. [37]).

According to Young's equation, the contact angle is a parameter defined by a local equilibrium condition governed by interfacial tensions:

$$\cos\theta = \frac{\gamma_{sv} - \gamma_{sl}}{\gamma_{lv}}. \tag{3}$$

It should be noted that Young's equation is only applicable when thermodynamically meaningful contact angles are obtained [35]. In that case, Eq. (3) suggests that the observed increase in contact angles is a manifestation of the effect of the electric field on interfacial tensions. Due to the lack of mobility of the molecules of the solid, it is unlikely that a change in solid–vapor surface tension is the underlying reason for the shift in contact angles. The fact that the contact angle of alkanes, unlike that of alcohols, remains unchanged in the electric field further supports this idea. On the other hand, liquid molecules (particularly polar ones like alcohols) can be easily moved or aligned in the electric field. Therefore, it is believed that the observed shift in contact angles is a consequence of a change in liquid interfacial tensions (i.e., γ_{sl} and/or γ_{lv}).

Taking the solid–vapor surface tension as constant, the effect of the electric field on contact angles can be translated into corresponding effects in terms of liquid surface tensions using the equation of state for interfacial tensions [49,53],

$$\gamma_{sl} = \gamma_{lv} + \gamma_{sv} - 2\sqrt{\gamma_{lv}\gamma_{sv}}e^{-\beta(\gamma_{lv}-\gamma_{sv})^2}. \tag{4}$$

Equation (4) relates the solid–liquid surface tension, γ_{sl}, to liquid–vapor, γ_{lv}, and solid–vapor, γ_{sv}, surface tensions, where $\beta = 1.241 \times 10^{-4}$ $(\mathrm{mJ/m^2})^{-2}$ is an empirical constant [35]. Using the equation of state in conjunction with Young's equation yields

$$\cos\theta = -1 + 2\sqrt{\frac{\gamma_{sv}}{\gamma_{lv}}}e^{-\beta(\gamma_{lv}-\gamma_{sv})^2}. \tag{5}$$

This equation was employed to calculate liquid–vapor surface tension in the electric field.

Two different approaches were used for this purpose. In the first approach Eq. (5) was employed twice, for the data in the absence and presence of the electric field,

$$\theta^{o} = f(\gamma_{sv}, \gamma_{lv}^{o}), \tag{6}$$

$$\theta^{e} = f(\gamma_{sv}, \gamma_{lv}^{e}), \tag{7}$$

where the function f represents the relationship described by Eq. (5) and the superscripts ^{o} and ^{e} indicate the values in the absence or presence of an electric field, respectively. Liquid–vapor surface tensions in the absence of the electric field, γ_{lv}^{o}, were determined using a pendant drop configuration [55]. Therefore, in the set of Eqs. (6) and (7) the values of θ^{o}, θ^{e}, and γ_{lv}^{o} were experimentally measured and the quantities γ_{lv}^{e} and γ_{sv} are unknown. The liquid–vapor surface tension in the electric field was then calculated by solving this system of equations for γ_{lv}^{e}.

Table 4
The calculation of the effect of an electric field on surface tension of alcohols when an electric potential of 4.5 kV is applied

Liquid	θ^{o} (°)	θ^{e} (°)	γ_{lv}^{o} (mJ/m^2)	γ_{lv}^{e} (mJ/m^2)	Percent of change in γ_{lv}
Hexanol	68.19	68.62	26.05	26.28	0.88
Heptanol	69.54	70.02	26.85	27.12	1.01
Octanol	71.09	71.67	27.50	27.83	1.20
Nonanol	71.82	72.46	27.55	27.93	1.38
Decanol	73.05	73.82	28.29	28.76	1.66
Dodecanol	74.48	75.40	29.41	30.00	2.01

Note. θ^{o} and θ^{e} are the contact angles obtained from the linear model at zero and 4.5 kV, respectively; γ_{lv}^{o} is the measured value of surface tension in the absence of the electric field; and γ_{lv}^{e} is the liquid–vapor surface tension calculated from the equation of state.

Table 4 summarizes the above calculations for alcohols at an electric potential of 4.5 kV. The first two columns show the contact angle results at zero and 4.5 kV electric potential, respectively. The contact angles were obtained from the fitted regression line (i.e., the value of the regression line at the corresponding electric potential) to minimize the effect of random experimental error. The third column shows the measured values of the liquid surface tension, γ_{lv}^{o}. The last two columns show the calculated surface tension in the electric field, γ_{lv}^{e}, and the percentage change in the surface tension, respectively. Table 4 suggests that the surface tension of alcohols increases in the electric field by one or two percent, depending on the chain length of the molecules. That is, the effect of the electric field is more significant for liquids with longer molecules. This increase is in agreement with the results obtained from a recent surface tension methodology, i.e., ADSA-EF [37]. Early results using ADSA-EF suggested an increase of about 1% in the surface tension of water when an electric field with the magnitude of 10^6 V/m is applied.

As a second alternative approach, the values of γ_{lv}^{e} can be calculated by employing the literature value of γ_{sv} along with Eq. (7). Recent studies have shown that the best value for the surface tension of Teflon AF 1600 (used in this study) is 13.61 mJ/m^2 [54]. This value was calculated from an Axisymmetric Drop Shape Analysis using liquids with bulky molecules and is believed to be accurate [49,54]. By substituting the literature value of γ_{sl} and the measured values of θ^{e} into Eq. (7) it follows that the surface tension increases by 0.87% for hexanol and by 1.97% for dodecanol. These quantities show good agreement with the results of Table 4, which were calculated using the first approach. The small deviation between the results of the two methods may be due to the fact that they are based on different sets of experimental data for zero electric field. The first method is based on the contact angles measurements of alcohols using the APF technique, while the second approach is based on the contact angle measurement of bulky molecules using ADSA.

The operative mechanism causing the above change in the interfacial tensions must be due either to an "interfacial effect" or a "bulk effect." An interfacial effect is operative

when the distribution of charge or material over the liquid–vapor interface is changed due to the electric field. That is, when the positive or negative head of liquid molecules (depending on the polarity of the electric field) points towards the interface as a result of the alignment of the polar molecules in the electric field. Alternatively, a bulk effect may be operative when bulk properties of the liquid are changed due to a rearrangement of molecules in the bulk phase. Electrostriction [56,57], i.e., an increase in the density of liquid due to an applied electric potential, is a possible example. The fact that the polarity of the electric field does not have an effect the contact angle (or surface tension) results suggests that a bulk effect is the operative mechanism. In this case both liquid–vapor and solid–liquid surface tensions are expected to be changed in the electric field. This is the most likely scenario and is entirely compatible with the assumptions underlying Eqs. (4) and (5).

However, if one were to assume that the electric field only affected the liquid–vapor surface tension, γ_{lv}, and the solid–liquid surface tension, γ_{sl}, were to remain unchanged (an unlikely scenario), then $\gamma_{\mathrm{lv}}^{\mathrm{e}}$ would be derived from Young's equation,

$$\gamma_{\mathrm{lv}}^{\mathrm{e}} = \gamma_{\mathrm{lv}}^{\mathrm{o}} \frac{\cos\theta^{\mathrm{o}}}{\cos\theta^{\mathrm{e}}}. \tag{8}$$

By substituting the measured values on the right-hand side of Eq. (8) one would calculate a surface tension increase of from 1.91% for hexanol to 6.14% for dodecanol. This is a much larger change compared to the values of Table 4. This value appears to be unreasonably large.

4. Summary

1. A methodology was employed that is believed to produce thermodynamically meaningful contact angles. It includes employing an advanced measuring technique (i.e., Automated Polynomial Fitting, APF), preparation of high-quality solid samples, advancing the three-phase line during measurements, and examining the patterns and trends of the observations for each run.
2. Experiments were carried out at different voltages. At each voltage nine replications were conducted. The overall mean of the results suggested an increase in the contact angles with increasing magnitude of the electric field.
3. Thorough statistical tests were conducted to examine the significance of the observed trends. The results indicated that the trends observed for alcohols are significant, while the trends calculated for alkanes could be due to random experimental error. Hence, it was concluded that the polarity of liquids is an underlying factor in the effect of electric fields on contact angles.
4. It was found that the shift in contact angles of alcohols in an electric field is larger for liquids with long-chain molecules.
5. The effect of the direction of the electric field was investigated by reversing the polarity of the capacitor. It was found that the direction of the electric field does not play a role in the observed effects. This finding suggests that the observed increase in contact angles in the electric field is due to a bulk effect rather than an interfacial effect.
6. Using the equation of state for interfacial tensions, the observed increase in contact angles was translated into a corresponding change in the liquid surface tensions. The results indicate that the surface tension of alcohols increases by one or two percent (depending on the chain length of the molecule) when an electric potential of 4.5 kV is applied. This voltage causes an electric field of the order of 10^6 V/m at the drop surface.

Acknowledgments

This investigation was financially supported by the Canadian Space Agency (Contract 9F007-006051/001/ST) and a University of Toronto Open Fellowship.

References

[1] T.G. Twardeck, IBM J. Res. Dev. 21 (1977) 31.
[2] M. Cloupeau, B. Prunet-Foch, J. Electrostat. 25 (1990) 165.
[3] I. Hayati, A.I. Bailey, T.F. Tadros, J. Colloid Interface Sci. 117 (1987) 205.
[4] B.K. Ku, S.S. Kim, J. Electrostat. 57 (2003) 109.
[5] A. Bologa, A. Bologa, J. Electrostat. 51 (2001) 470.
[6] K. Asano, K. Yatsuzuka, J. Electrostat. 46 (1999) 69.
[7] C. Schmitt, M. Lebienvenu, J. Mater. Process. Technol. 134 (2003) 303.
[8] C.H. Byers, A. Amarnath, Chem. Eng. Prog. (1995) 63.
[9] A.J. Pederson, L.M. Ottosen, A.J. Villumsen, J. Hazard. Mater. 100 (2003) 65.
[10] T. Nemoto, M. Ishikawa, H. Momota, Fusion Eng. Des. 63–64 (2002) 501.
[11] J.S. Eow, M. Ghadiri, Chem. Eng. Proc. 42 (2003) 259.
[12] K. Tang, R.D. Smith, J. Am. Soc. Mass Spectrom. 12 (2001) 343.
[13] G. Atungulu, Y. Nishiyama, S. Koide, Biosys. Eng. 85 (2003) 41.
[14] M. Tuller, D. Or, J. Hydrol. 272 (2003) 50.
[15] J.S. Chang, J. Electrostat. 57 (2003) 273.
[16] M. Cloupeau, B. Prunet-Foch, J. Electrostat. 25 (1990) 165.
[17] G. Joffre, B. Prunet-Foch, S. Berthomme, M. Cloupeau, J. Electrostat. 13 (1982) 151.
[18] O.A. Basaran, L.E. Scriven, J. Colloid Interface Sci. 140 (1990) 10.
[19] M.T. Harris, O.A. Basaran, J. Colloid Interface Sci. 161 (1993) 389.
[20] M.T. Harris, O.A. Basaran, J. Colloid Interface Sci. 170 (1995) 308.
[21] Y. Nakamura, K. Kamada, Y. Katoh, A. Watanabe, J. Colloid Interface Sci. 44 (1973) 517.
[22] Y. Nakamura, M. Matsumoto, K. Nishizawa, K. Kamada, A. Watanabe, J. Colloid Interface Sci. 59 (1977) 201.
[23] M. Sparnaay, J. Surf. Sci. 1 (1964) 213.
[24] R. Digilov, Langmuir 16 (2000) 6719.
[25] W.J.J. Welters, L.G.J. Fokkink, Langmuir 14 (1998) 1535.
[26] M. Vallet, B. Berge, L. Vovelle, Polymer 37 (1996) 2465.
[27] M. Vallet, M. Vallade, B. Berge, Eur. Phys. J. B 11 (1999) 583.
[28] P.Y. Chiou, H. Moon, H. Toshiyoshi, C.J. Kim, M.C. Wu, Sens. Actuat. 104 (2003) 222.

[29] J. Lee, H. Moon, J. Fowler, T. Schoellhammer, C.J. Kim, Sens. Actuat. 95 (2002) 259.
[30] C. Quilliet, B. Berge, Curr. Opin. Colloid Interface Sci. 6 (2001) 34.
[31] H.J.J. Verheijen, M.W.J. Prins, Langmuir 15 (1999) 6616.
[32] G. Lippmann, Ann. Chim. Phys. 5 (1875) 494.
[33] R.J. Good, in: R.J. Good, R.R. Stromberg (Eds.), Surface and Colloid Science, vol. 11, Plenum, New York, 1979, p. 1.
[34] C.N.C. Lam, J.Y. Lu, A.W. Neumann, in: K. Holmberg, M.J. Schwuger, D.O. Shah (Eds.), Handbook of Applied Surface and Colloid Chemistry, in press.
[35] D.Y. Kwok, A.W. Neumann, Adv. Colloid Interface Sci. 81 (1999) 167.
[36] D.Y. Kwok, A. Leung, C.N.C. Lam, D. Li, R. Wu, A.W. Neumann, J. Colloid Interface Sci. 206 (1998) 44.
[37] A. Bateni, S.S. Susnar, A. Amirfazli, A.W. Neumann, Langmuir 20 (2004) 7589.
[38] C.F. Hayes, J. Phys. Chem. 79 (1975) 1689.
[39] I. Morcos, J. Electrostat. 5 (1978) 51.
[40] Y. Morimoto, K. Saheki, Jpn. J. Appl. Phys. 18 (1979) 1239.
[41] Y.A. Shchipunov, A.F. Kolpukou, Adv. Colloid Interface Sci. 35 (1991) 331.
[42] J. Goodisman, J. Phys. Chem. 96 (1992) 6355.
[43] L. Liggieri, A. Sanfeld, A. Steinchen, Physica A 206 (1994) 299.
[44] M. Sato, N. Kudo, M. Saito, IEEE Trans. Ind. Appl. 34 (1998) 294.
[45] A. Sanfeld, Phil. Trans. R Soc. London Ser. A 356 (1998) 819.
[46] DuPont Inc., Product Information: Teflon AF Amorphous Fluoropolymers, 204103D, February 1998.
[47] W.H. Buck, P.R. Resnick, Teflon AF Amorphous Fluoropolymers Technical information: Properties of Amorphous Fluoropolymers Based on 2, 2-Bistrifluoromethyl-4, 5-Difluoro-1, 3-Dioxole, presented at the 183rd Meeting of the Electrochemical Society, Honolulu, HI, May 17, 1993.
[48] C.N.C. Lam, R. Wu, D. Li, M.L. Hair, A.W. Neumann, Adv. Colloid Interface Sci. 96 (2002) 169.
[49] H. Tavana, C.N.T. Lam, K. Grundke, P. Friedel, D.Y. Kwok, M.L. Hair, A.W. Neumann, J. Colloid Interface Sci. 279 (2004) 493.
[50] A. Bateni, S.S. Susnar, A. Amirfazli, A.W. Neumann, Colloids Surf. A 219 (2003) 215.
[51] R.E. Walpole, R.H. Myers, S.L. Myers, K. Ye, Probability and Statistics for Engineers and Scientists, Prentice–Hall International, Englewood Cliffs, NJ, 2002, p. 364.
[52] F.K. Wohlhuter, O.A. Basaran, J. Fluid Mech. 235 (1992) 481.
[53] J.K. Spelt, D. Li, in: A.W. Neumann, J.K. Spelt (Eds.), Applied Surface Thermodynamics, Dekker, New York, 1996, p. 239.
[54] H. Tavana, R. Gitiafroz, M.L. Hair, A.W. Neumann, J. Adhes. 80 (2004) 705.
[55] O.I. del Rio, A.W. Neumann, J. Colloid Interface Sci. 196 (1997) 136.
[56] J.C. Rasaiah, D.J. Isbister, G. Stell, J. Chem. Phys. 75 (1981) 4707.
[57] Y.M. Shkel, D.J. Klingenberg, J. Appl. Phys. 80 (1996) 4566.